

RAL 93090
COPY 2 R61 ER
Acc: 221607

RAL-93-090 Science and Engineering Research Council

Rutherford Appleton Laboratory

Chilton DIDCOT Oxon OX11 0QX

RAL-93-090

AP, INST

The Experimental Characterisation of Gas Microstrip Detectors: I. Gain Characteristics

J E Bateman and J F Connolly

December 1993

Science and Engineering Research Council

"The Science and Engineering Research Council does not accept any responsibility for loss or damage arising from the use of information contained in any of its reports or in any communication about its tests or investigations"

THE EXPERIMENTAL CHARACTERISATION OF GAS MICROSTRIP DETECTORS

I. GAIN CHARACTERISTICS

J E Bateman and J F Connolly
Rutherford Appleton Laboratory, Chilton, Didcot, OX11 0QX, U.K.

The results of a programme of research into the experimental properties of gas microstrip detectors are reported. In this report information on the gain characteristics of the devices is presented.

1. INTRODUCTION

Since its introduction by Oed [1], the gas microstrip detector (GMSD) has been studied by several groups for potential applications in high energy physics, space science, materials science and medicine.[2-8] The GMSD is a form of the gas proportional counter in which an extremely precise pattern of metallisation is laid down on an insulating substrate using standard microlithographic techniques. The pattern consists of interleaved narrow (typically $10\mu\text{m}$) and wide (typically $100\mu\text{m}$) metal strips separated by (typically) around $100\mu\text{m}$ strips of insulating substrate. Application of a few hundred volts between the anode and cathode strips in a suitable gas atmosphere results in amplification factors of up to 10000 for any free electrons captured by the anode. Figure 1 shows a typical detector structure with a drift electrode spaced a few millimeters away from the lithographic plate to define the active volume of the detector.

As a potential replacement for the multiwire proportional counter (MWPC) the GMSD has several attractions. First, independent detectors can be made on a pitch of 0.25mm or less; second, the positional accuracy of the electrodes essential for all gas detectors can be achieved easily and without the demand for structural strength which wire tensions impose on the MWPC; third, the very small anode-cathode gap leads to sub-microsecond positive ion transit times thus permitting count rate densities two orders of magnitude higher than is possible with a wire counter. The excellent spatial resolution ($< 30\mu\text{m}$) has been demonstrated in high energy particle tracking [3] and the structural precision has permitted excellent energy resolution [5].

The undoubted potential of the GMSD was vitiated throughout its early development by the presence of gain instabilities which are severely aggravated by high counting rates so robbing it of its one great advantage over a wire counter. This gain instability was quickly determined to be a result of the effect of the very high electric fields at the edge of the anode on the substrate material. In extensive tests with conventional glasses (pyrex, etc) [9] the well-known ionic polarisation effects of such materials were shown to be responsible. When it was suggested [10,11] that semiconducting glasses might offer a more stable substrate we immediately obtained samples and produced GMSDs on them. The resulting detectors showed a degree of stability and reproducibility which, for the first time, made systematic measurements on our GMSDs possible. The following results are taken mainly on devices fabricated on semiconducting glass.

Test detectors were fabricated using the basic pattern of figure 1. In the lithography 20 anodes (60mm long) are bussed together with a connecting pad at the outboard end and the corresponding cathodes are similarly treated. This results in an active detector area of 6mm x 60mm with this pattern repeated five times on a standard 100mm x 100 glass plate giving five independent detectors. The metalisation was generally aluminium and two distinct types of semiconducting glass were used - Schott S8900 ($10^{11}\ \Omega\text{-cm}$) and Pestov P9 ($10^9\ \Omega\text{-cm}$) [9]. The processing was mainly carried out by VTT in Finland.

In order to be able to make use of smaller glass samples, a test pattern was designed which restricted the length of the active detector area to 15mm and so accommodated the structures within an area of 50mm x 50mm.

The gas mixtures used were either argon+20% methane (premixed) or argon+25% isobutane, flowed through the detector box. X-ray stimulation was derived from a Cu-anode X-ray

generator.

2. GAIN CHARACTERISTICS

The operating potentials used in our tests were generally $V_a=0V$, $V_c=-600V$ to $-800V$ and $V_d=V_c$ to $-3000V$ (figure 1). These potentials result in an electric field configuration in the gas above the plate of the form illustrated in figure 2. (This shows the field lines in a plane transverse to the strip pattern on the plate.) The characteristic of this pattern is that the field configuration divides into two clearly defined regions, a dipole region within one pattern pitch of the plate and a drift region with an approximately uniform electric field filling the rest of the conversion space. When $V_d=V_c$, the mean attractive potential for electrons of our metal strip pattern can be estimated as $\approx V_c/3$ (assuming the potential across the plate is graded by the conducting substrate) so giving an effective electron drift field of $(V_d - 2V_c/3)/d$, where d is the separation of the drift electrode and the plate. A standard test configuration for gain tests is to set $V_d=V_c$, so giving a collecting field of $V_c/3d$.

2.1 A Basic Gain Formula

An avalanche occurs when a cloud of electrons from (say) an x-ray conversion in the drift space arrives in the high field region just above the anode. The gas gain (G) is as usual given by

$$\ln G = \int \alpha dx$$

along the path of the electrons (α is the Townsend coefficient). This demands a knowledge of the electric field, which, in this case must be obtained by numerically integrating Laplace's equation. This has been done by Florent et al [12] and gain curves calculated. For practical analysis of the behaviour of GMSD's a simpler approach is required. It has been shown elsewhere [13] that a simple model for the gain process in a cylindrical wire counter yields a semi-empirical gain formula which fits the behaviour of different types of flowing gas counter well in the region of ambient thermodynamic variables.

The gain formula is:

$$\ln G = \frac{V}{A} \exp(-B/V) \quad (1)$$

where V is the anode-cathode potential, A is a constant and B is a linear function of the ambient variables ($B = aP/T + b$). In an ideal world, the variables A , a and b are dependent only on the gas and the dimensions of the strip pattern. Due to substrate interactions things are more complicated than this.

Equation (1) is found to give an excellent fit to any GMSD gain curve so far measured and the range of fit exceeds two decades in gain. Figure 3 shows the fits to gain curves for GMSD's

fabricated on Tempax (borosilicate glass) and P9 semiconducting glass ($V_d = V_c$). As figure 3 shows, when the gain is plotted logarithmically against V_c , a virtually straight line results. A curious (and useful) feature of the log-gain curves is that the slope is almost a universal constant independent of gas, substrate or anode width, with the gain doubling for every 45V. Variations in the significant parameters simply moves the line up and down the log-gain axis.

2.2 The Effect of Detector Geometry on the Gain

Since it would clearly be useful to have a semi-empirical description of the dependence of the gain on the strip dimensions an attempt was made to extend the analogy with the wire counter by including the typical dimensional term $\ln(b/a)$ (a is the anode radius and b the cathode radius in the cylindrical configuration). The following modification of equation (1) was fitted to some experimental data of our own and the modelled gain curves of Florent et al [12] based on their accurate field calculations:

$$\ln G = \frac{V}{p [\ln(b/a)]^c} \exp\left\{-\frac{a[\ln(b/a)]^c}{qV}\right\} \quad (2)$$

Where p , q and c are constants obtained by fitting to experimental data. As figures 4a and 4b show this function adequately describes the behaviour of the gain as the anode width varies (and the anode-cathode gap is held constant). The approximation holds good as long as the anode-cathode gap does not become too small. As figure 4c shows, the agreement with the Florent data breaks down dramatically if the gap is less than $75\mu\text{m}$.

The formula clearly cannot take account of the field modifications caused by the substrate and so can only be applied to a single substrate and gas at a time. (Figure 5 shows this effect strongly; the P9 plate has the same pattern and operates in the same gas as the S8900 plate but the gain is a factor of two lower due to the grading effect of the lower resistivity on the electric field in the anode-cathode gap.) However, it does give useful insights such as the decrease in the gain at low anode widths, which results from the anode width approaching the mean free path of the avalanche process. It would appear that the minimum practical anode width is around $5\mu\text{m}$.

2.3 The Effect of the Drift Field

It is obvious from the field pattern shown in figure 2 that the two field regions are reasonably decoupled. This results in the drift field (and so V_d) having very little effect on the gas gain. Figure 6 shows the relative gas gain of an GMSD (operating in argon+20% methane) as a function of $V_d - V_c$ at a variety of V_c values. The gain varies only weakly (and approximately linearly) with V_d showing a slope of $\approx 2.5\%$ per 100V. The slope changes very little with V_c , so for practical purposes V_c and V_d are decoupled. Further, the slope is very similar for different gases: in argon+25%isobutane the slope is $\approx 1.8\%/100V$.

Using a reasonably high value of V_d (several kV) is advantageous for several reasons:

(a) a factor of ≈ 1.5 increase in the gain can be achieved above the value at which the plate

structure reaches its limit

(b) the drift time of the initial ionisation can be significantly reduced (and thus the timing resolution of the GMSPD increased)

(c) the rate performance of the GMSPD is marginally improved

The weak dependence of the gas gain on the drift field has a beneficial effect on GMSPD design by removing any requirement for high precision in the drift electrode structure. The gain is determined essentially by the lithographic pattern, the precision of which is guaranteed by the production process.

3. GAIN UNIFORMITY

3.1 Substrate Effects

As reported in our earlier work [9] we found that the gain of GMSPD's fabricated on insulating or semi-insulating substrates could vary by a factor of two or more over the area of the 100mm x 100mm plate. This was clearly due to the physico-chemical state of the surface after processing since it could be strongly influenced by a mild bake. Early devices fabricated on S8900 in the Central Microstructure Facility at RAL showed an immediate improvement in this respect. However, even better results were obtained when an S8900 plate was processed by VTT in such a way as to minimise the exposure of the glass to the etchant. Figure 7 shows the gain measured by a 1mm diameter x-ray beam as it was scanned the whole length (60mm) of a test section. This level of uniformity is very acceptable for any application we can foresee and is maintained over the whole of the active area of the plate.

3.2 Geometry Effects

Equation (2) facilitates an exploration of the effect on the gain of an GMSPD produced by tolerances in the lithographic process. Figure 8 shows the measured width at intervals along one anode strip on a particular plate, and above it the corresponding gain calculated from equation (2) (the standard strip geometry of figure 1 is assumed). As can be seen, at a gain of 1762 the RMS gain fluctuations (3.8%) are of the same order as those in the anode width (3.1%). Figure 8 shows that permissible anode width tolerances can be a relatively poor $0.3\mu\text{m}$ (compared to the best that microlithography can achieve) and still give acceptable gain uniformity.

The actual gain uniformity of plate 92 (figure 8) was drastically worse than that calculated [9] again illustrating the importance of the substrate in defining the gain. The excellent uniformity shown by the S8900 detector shown in figure 7 illustrates high quality lithography as well as a uniform substrate. The deviations at the ends probably reflect edge effects from the ends of the drift cathode which (in this detector) is only 3mm from the plate surface.

3.3 Pulse Height Resolution

GMSD's that exhibit variable gain across the active area also show a similar instability in the pulse height resolution. We are pleased to report that detectors fabricated with semiconducting glasses exhibit excellent and uniform pulse height resolution of $\approx 12\%$ FWHM for Cu K x-rays. To first order, this figure does not seem to be affected by position, gas mixture or the bias conditions (i.e. variation of V_d) provided the gas is adequately pure.

4. GAIN STABILITY

4.1 Substrate Effects

Ionic polarisation effects in the substrate lead to initial drift of the gain when the bias is first applied (particularly at high counting rates). The two semiconducting glasses in our devices show a small ($\approx 5\%$) gain drop within 20 seconds of applying the bias, but stabilise within a minute showing no further effects. The characteristic leakage current decrease under bias typical of ionic conductors is not observed, rather the leakage current follows the ambient temperature according to the relation $\sigma = \sigma_0 \exp(-W/kT)$ (where W is an activation energy). Because of the load resistor included for safety reasons in the HT bias circuit, the temperature dependence of the leakage current introduces a negative gain shift with temperature. The GMSDs fabricated on semiconducting glasses show (essentially) linear I/V curves with the S8900 detectors drawing 80nA/cm^2 and the S9 detectors $8\mu\text{A/cm}^2$.

Figure 9 shows a plot of the leakage current of one of the small test sections on P9 glass as a function of $1000/T$. The current shows a very steep dependence on temperature (the activation energy is 0.47eV) with an extra microamp of current for only a three degree increase in temperature. With a few $\text{M}\Omega$ load resistor the resulting gain loss is significant. Equation (1) can be used to estimate the gain changes induced by an unstable HT:

$$dG/dV = G \ln G (1 + B/V)/V$$

At a gain of 1000 in argon+20% methane this relation predicts $dG/dV = 17.4 (\text{V}^{-1})$ i.e. a 17.4% gain drop would occur over $3C$ if a $1\text{M}\Omega$ load resistor were used.

4.2 Ambient Stability

As equation (1) indicates, the gain of any flowing gas counter fluctuates with the ambient pressure and temperature. Previous studies [13] showed that the sensitivity of the gain process to q ($=P/T$) depended on the number of mean free paths in the avalanche. This led to the conclusion that our GMSD with its $10\mu\text{m}$ wide anode should show good stability against ambient fluctuations (which could prove very helpful in the design of large experiments). In order to verify this we monitored the gain of an S8900-based GMSD over a period of two weeks. In order to evaluate the constants a and b we plotted $\ln(\ln G)$ as a function of q when the applied HT was kept constant. Rearranging equation (1) shows that:

$$\ln(\ln G) = \{\ln(V/A) - b/V\} - aq/V \quad (4)$$

This gives a linear graph against q and the gain curve must be plotted to find the value of A . Figure 10 shows the plot of the experimental data and the fit. Using the fit parameters we arrive at values for the constants of equation (1) for this counter of: $A = 55.39V$, $a = 56.11VK/mb$ and $b = 155.79V$. In more familiar terms we have gain coefficients of $dG/dP = -0.3\%/mb$ at $20C$ and $dG/dT = +1\%/C$ at $1000mb$ when the gain is 570 . A useful relation for the gain coefficients can be obtained by differentiating (1):

$$TdG/dT + PdG/dP = 0$$

This calibration can, of course, be used to servo the HT and keep the gain constant against ambient changes.

5. NOISE

When studies of GMSDs with semiconducting glass substrates began, we immediately noticed an increase in pulse noise as the gain approached useful values (> 1000). Initial tests with the S8900 glass showed that the noise was minimised when the backplate electrode was held at $\approx 0.5V_c$. (With semi-insulating substrates we generally set this potential to V_c .) The substrate P9 showed even greater noise problems and forced further tests to discover its source. It was found that if the semiconducting substrates were isolated from the backplate electrode the noise completely disappeared. This finding indicates that the noise is a result of the injection of current into this electrode from the substrate as a result of its low resistivity.

At the very high gains (> 20000) made possible with the "robber bar" modification described below, low amplitude pulse noise begins to appear (as is usual in all gas counters) and in the case of P9 glass, if the ambient temperature is above $\approx 18C$, the noise can begin to increase with time in a manner reminiscent of the thermal runaway familiar in the operation of channel electron multipliers (which are also made of semiconducting glass). We have not explored this phenomenon in detail, but we believe that it is an indication that the resistivity of P9 glass ($10^9 \Omega\text{-cm}$) is just too low for practical detectors.

6. GAIN LIMITATION

The maximum stable gain achievable with any given GMSD detector has always been a very variable and unpredictable quantity. The fact that the maximum gain increases (in the usual way) with the strength of the quencher indicates that the usual limiting processes of UV-stimulated cathodic emission are at work. Unfortunately, our new stable GMSD's on semiconducting glass showed much lower maximum gains than we obtained on the pyrex glass and threatened the usefulness of the new glass.

Early experience with the GMSD's showed that a common source of breakdown was the tip of the cathode metallisations where they terminated at the anode end of the detector (figure 11).

Attempts have been made to propose different configurations of the cathode end to try to reduce the electric field at the edge [14] but without conspicuous success. In accordance with normal high-field engineering principles we graded the widths of anode and cathode strips so that when the cathodes terminated both anode and cathode strips had equal width. However, this led to no significant improvement in the maximum permissible gain.

Potting the critical region of the plate in epoxy resin is an easy option which we have found to be unsatisfactory in the long term due to deterioration of the insulating properties over time. A coating of silicon dioxide certainly forms an excellent insulator but increases costs by introducing a further processing step.

It occurred to us that the problem could be solved by redirecting the field lines from the continuing anodes to an auxiliary negative electrode brought up close (a few hundred microns) and parallel to the plate just over the region where the cathode strips terminate. This "robber bar" steals the field lines from the cathode ends and so reduces the electric field in the critical region. Clearly the gas region under the robber bar is an active counter volume; but by keeping it narrow and shallow undesirable amplified noise should be minimised.

A prototype robber bar was made from a 3mm wide strip of copper-clad glass fibre board and spaced $400\mu\text{m}$ above the cathode ends (in the drift space). Provision was made to connect an independent negative HT to the copper surface which faced the plate. The GMSD under study was the small device on P9 glass operated with an argon+20% methane gas.

Figure 12 shows the gain curves obtained from the counter with three different potentials on the robber bar. With $V_{rb}=0$ the maximum gain was 584 ($V_c=-600\text{V}$); with $V_{rb}=-700\text{V}$ the maximum gain increased to 1346 ($V_c=-650\text{V}$) and with $V_{rb}=-1200\text{V}$ a gain of 2373 was attained at $V_c=-690\text{V}$. In order to check for any influence of the robber bar on the spatial response of the detector, a scan perpendicular to it was made as figure 13 shows. The very slight gain rise (about 1%) towards the left (the robber bar side) shows that some very slight but unimportant effect is being felt. It is clearly important not to distort the drift field unnecessarily.

It is hoped that by reducing the robber bar to plate gap to around $200\mu\text{m}$ V_{rb} will be able to be set at V_c , thus removing the need for a third bias potential.

Changing the gas to argon+25%isobutane further improves the maximum gain as figure 14 shows. The maximum gain obtained from this GMSD was just over 30000.

7. CONCLUSIONS

The availability of semiconducting glass substrate material has permitted the fabrication of GMSD's with stable gain properties which we have characterised. Using two glass types of bulk resistivity 10^{11} and $10^9 \Omega\text{-cm}$ respectively we have demonstrated uniform and stable gain characteristics. Due to the high leakage current we favour a minimum resistivity of $10^{10} \Omega\text{-cm}$ for practical detectors. (At very high gains there was evidence of incipient thermal runaway in the P9 glass when the ambient temperature rose above 18C .)

Practical gain formulae have been derived which permit the comparison of various aspects of the gain performance of GMSD's between devices (within the limitations set by the substrate effects).

By introducing an auxiliary electrode (the "robber bar") we have obtained stable gains of up to 30000 in GMSD's fabricated on semiconducting glass without the need to pot portions of the detector surface.

ACKNOWLEDGEMENTS

We are particularly indebted to Yu N Pestov of the Budker Institute of Nuclear Research, Novosibirsk for supplying us with the samples of P9 glass used in the above programme and to Ilkka Suni and his colleagues at the Technical Research Centre of Finland (VTT) for their enthusiastic collaboration in the production of our GMSD plates. We would like to thank our colleagues Bernard O'Hagen, Adrian Walker and Aubrey Dobbs for their contributions to this work. Our thanks are also due to the staff of the RAL Central Microstructure Facility.

REFERENCES

1. A Oed, Nucl Instr & Meth A263 (1988) 351-359
2. F Angelini, R Bellazzini, A Brez, M M Massai, G Spandre and M R Torquati, Nucl Instr & Meth A283 (1989) 755-761
3. F Angelini, R Bellazzini, A Brez, M M Massai, G Spandre, M R Torquati, R Bouclier, J Gauden and F Sauli, IEEE Trans Nuc Sci 37 (no.2) 1990 112
4. F Hartjes, B Hendriksen and F Udo, Nucl Instr & Meth A289 (1990) 384
5. C Butz-Jorgensen, Rev Sci Instrum 63 (1) 1992 648
6. J E Bateman, J F Connolly, R Stephenson and J Morse, Proceedings of the European Workshop on X-ray Detectors for Synchrotron Radiation Sources, Aussois, France 1991
7. R Bouclier, J J Florent, J Gauden, A Pasta, L Ropelewski, F Sauli and L I Shekhtman, High flux operation of microstrip gas chambers on glass and plastic supports, presented at the Sixth International Wire Chamber Conference, Vienna, 1992, to be published in Nucl Instr & Meth
8. L I Shekhtman, High pressure gas avalanche chambers for medical radiology, presented at the Fourth International Conference on Application of Physics in Medicine and Biology, Trieste, 1992
9. J E Bateman and J F Connolly, Substrate-induced instability in gas microstrip detectors. RAL-92-085

10. G D Minakov, Yu N Pestov, V S Prokopenko and L I Shekhtman, Nucl Instr & Meth A326 (1993) 566-569
11. R Bouclier, G Million, L Ropelewski, F Sauli, Yu N Pestov and L I Shekhtman, Nucl Instr & Meth A332 (1993) 100-106
12. J J Florent, J Gaudaen, L Ropelewski and F Sauli, CERN report no. CERN-PPE/92-78
13. J E Bateman, Practical gain formulae for proportional counters, RAL-93-019
14. I Duerdoth, M Ibbotson, N Lumb, S Snow and R Thompson, Studies of breakdown in gas microstrip detectors, presented at the 3rd London Conference on Position Sensitive Detectors, Brunel University, September 1993

FIGURE CAPTIONS

Figure 1

A schematic section of the gas microstrip detector used throughout the studies reported in this paper.

Figure 2

A schematic representation of the electric field pattern in a gas microstrip detector showing the two distinct regions: the (low) parallel collection field filling most of the space between the drift electrode and the plate and the region of intense field in the vicinity of the anode (adapted from field plots given in reference [2]).

Figure 3

This shows the gain curves measured on two GMSD's with the same metal pattern, but on different substrate materials. $V_d = V_c$ and the gas is argon + 25% isobutane. The fit data to equation (1) is also shown.

Figure 4

(A) The fit of equation (2) to the gains from two GMSD's with anode widths of $10\mu\text{m}$ and $16\mu\text{m}$ on Tempax glass. The overall pitch of the pattern is maintained at $300\mu\text{m}$.

(B) The fit of equation (2) to the modelled gain data of Florent et al [12] for the gain of an GMSD as a function of the anode width.

(C) This shows the breakdown of the gain model of equation (2) as the cathode width is increased (at a constant pattern pitch). The equation fails rapidly when the anode-cathode gap is reduced below $\approx 75\mu\text{m}$.

Figure 5

The fits to the gains given by two identical mask patterns on different semiconducting substrates show the typical gain reduction caused by the grading of the electric field near the anodes by the lower resistivity substrate.

Figure 6

The gas gain relative to the condition $V_d = V_c$ is plotted as a function of $-(V_d - V_c)$ with various values of V_c for a GMSD fabricated on S8900 glass and operating in argon + 20% methane. The slopes of the straight line fits vary between 2.39%/100V and 2.6%/100V.

Figure 7

A scan of the gain of a beam chamber GMSD (every anode is independently read out) as a 1mm diameter x-ray beam is scanned along the length of an anode strip.

Figure 8

This shows a survey of the width of a single anode in one of the GMSD's fabricated at RAL (lower curve). The measured widths are inserted in the gain model (equation (2)) to see what are the predicted gain fluctuations (upper curve). The width tolerance of $0.27\mu\text{m}$ rms represents relatively poor lithographic accuracy but the consequent gain fluctuation (3.8%) is quite acceptable.

Figure 9

A plot of the leakage current of a section of the small test pattern (active length $\approx 14\text{mm}$ with 20 anodes in parallel) against $1000/T$ (the absolute temperature). The fit shows that the temperature behaviour is governed by the usual formula with an activation energy of 0.47eV. The resistance of the section at 20C is $87.3\text{M}\Omega$. The $30.42\text{M}\Omega$ constant in the fit formula is the series protection resistor.

Figure 10

This plot of $\ln(\ln(\text{gain}))$ against P/T shows the gain dependence of this particular GMSD on the ambient conditions when operated with flowing gas (argon + 20% methane).

Figure 11

This shows the positioning of the robber bar (dashed lines) over the ends of the cathode strips.

Figure 12

The increasing maximum gain permitted as the HT on the robber bar is increased is seen in the overlapping gain curves obtained from this GMSD (P9 glass).

Figure 13

Gain scans across the GMSD normal to the robber bar when it is at -1200V. The slight rise towards the robber bar (on the left) is $\approx 2\%$.

Figure 14

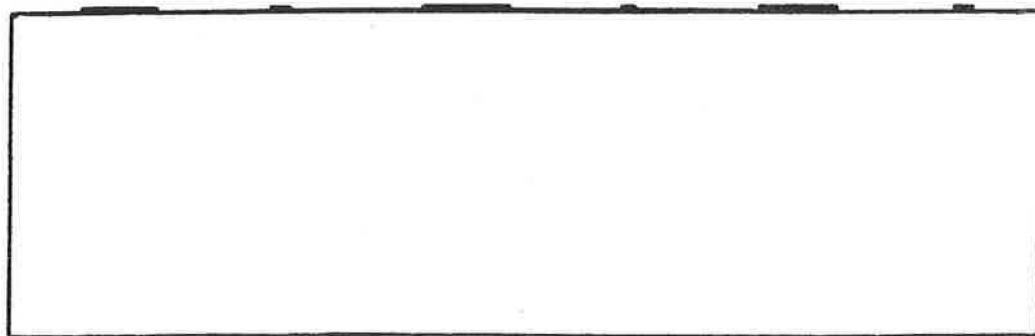
A gain plot (and fit) of the GMSD fitted with the robber bar when operated in argon + 25% isobutane.

Drift Electrode (Vd)

9 mm

Cathode (Vc) Anode (Va)

150 μm
90 μm 10 μm



1 mm

Back Plane (Vb)

Figure 1

FIGURE 2

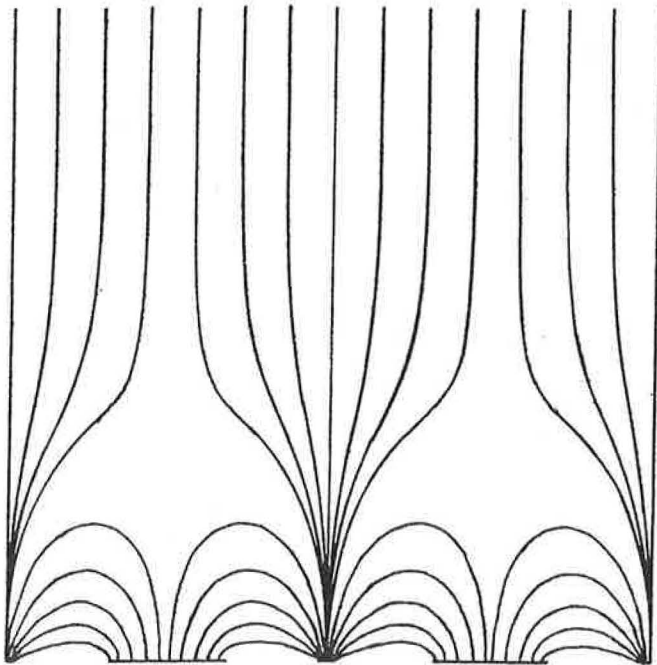
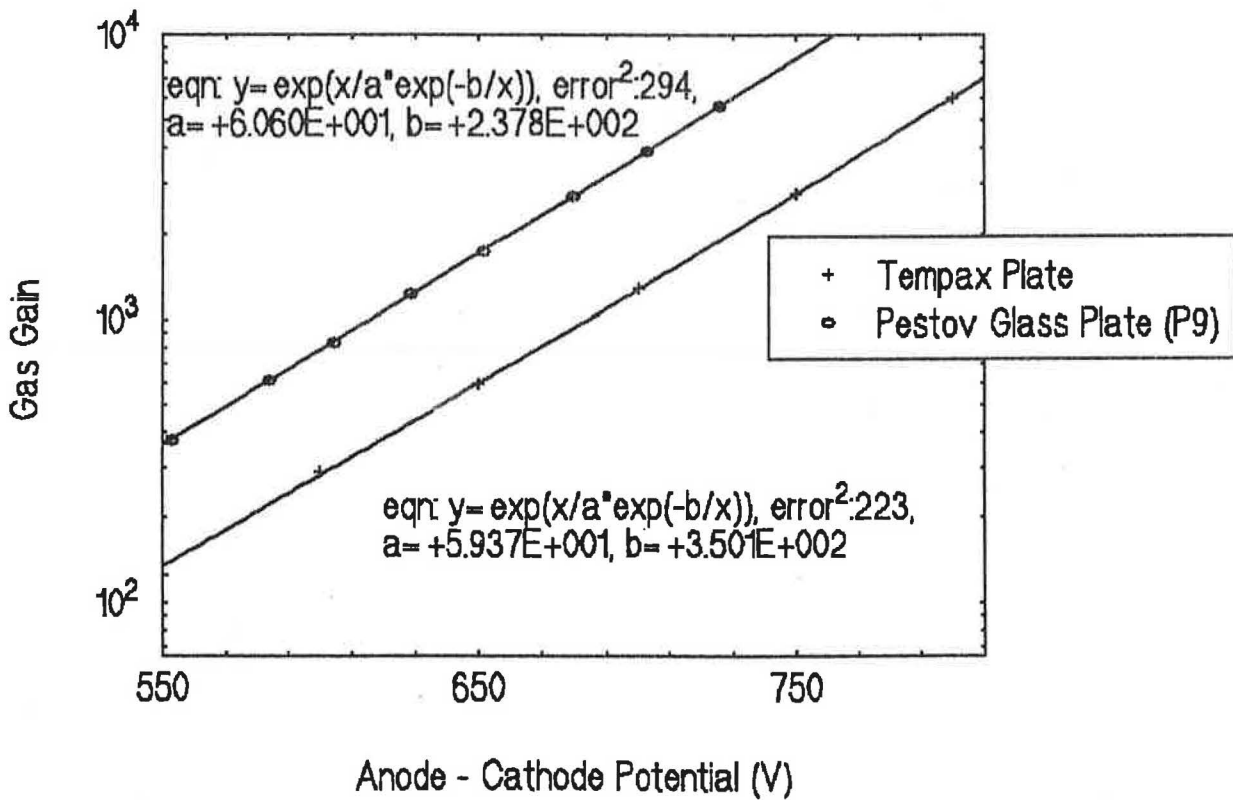


FIGURE 3



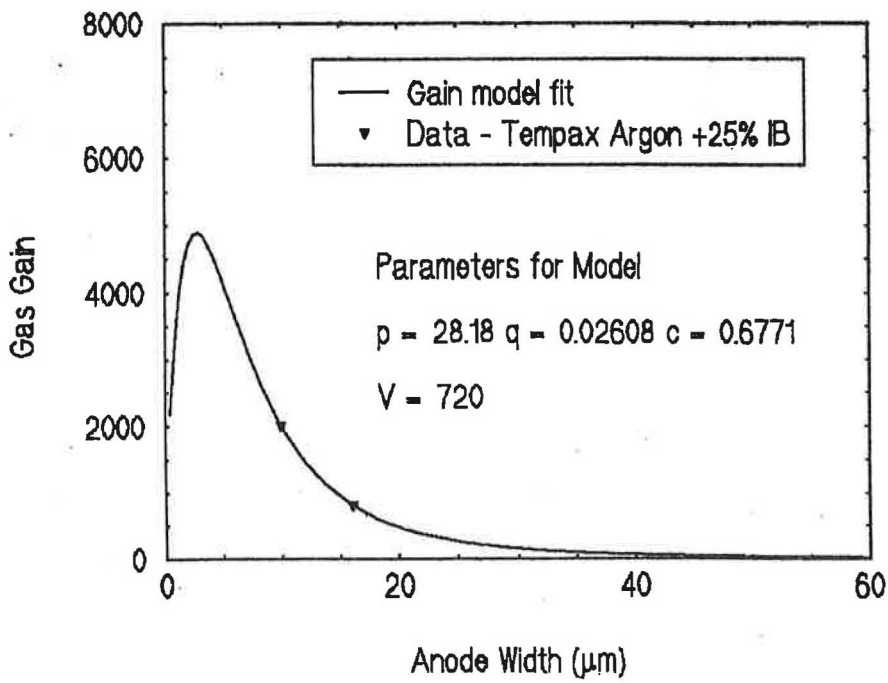


FIGURE 4A

FIGURE 4B

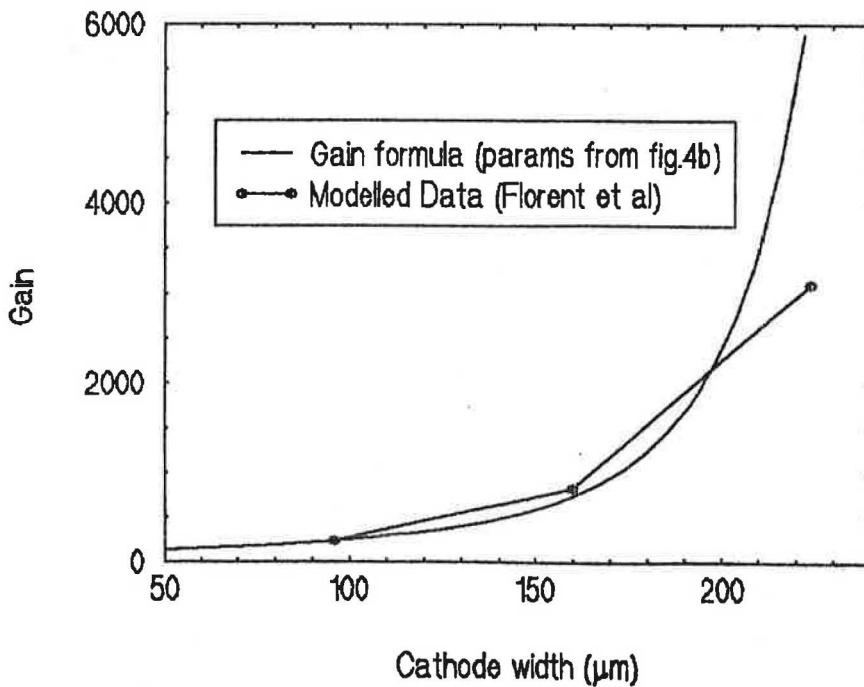
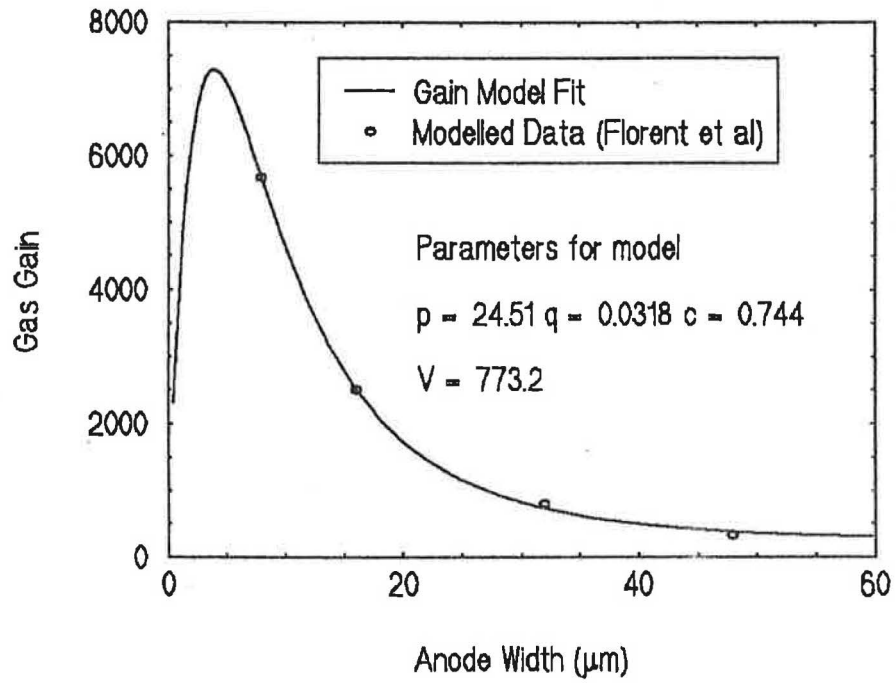


FIGURE 4C

FIGURE 5

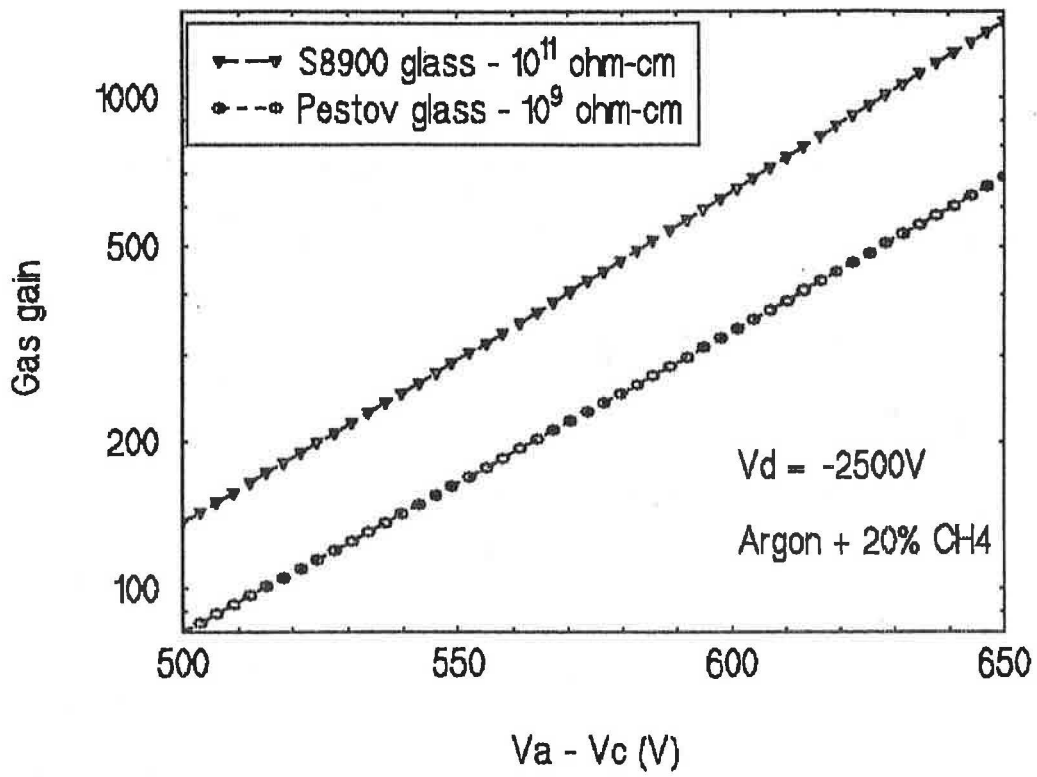


FIGURE 6

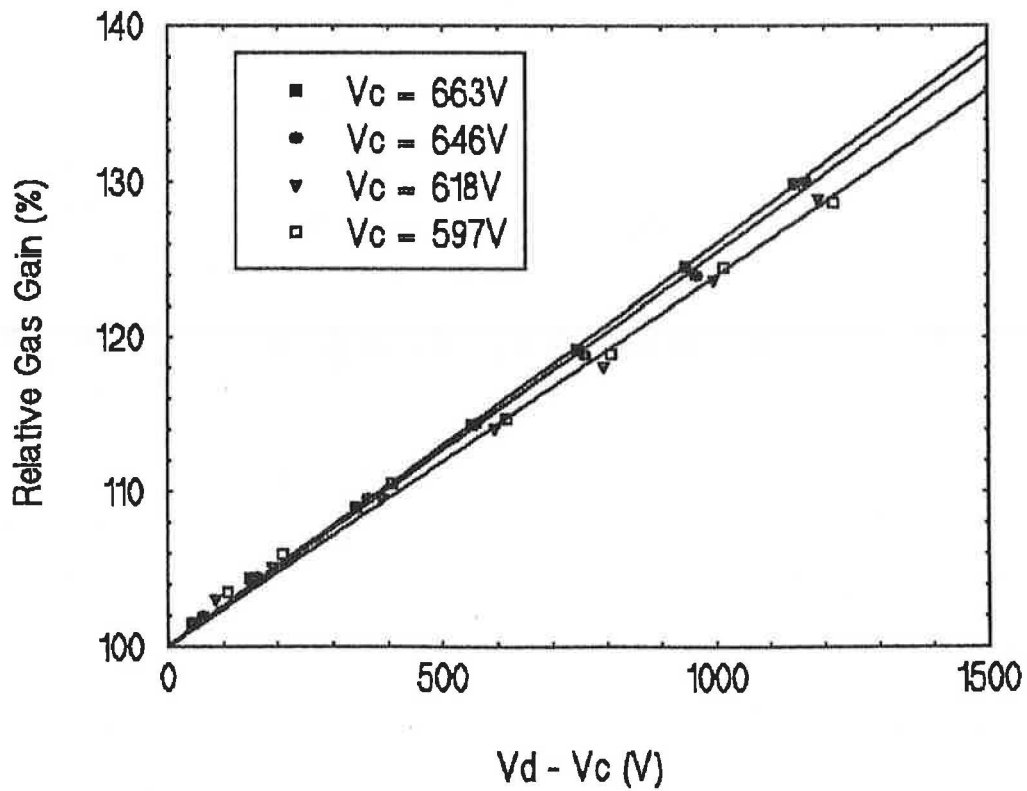


FIGURE 7

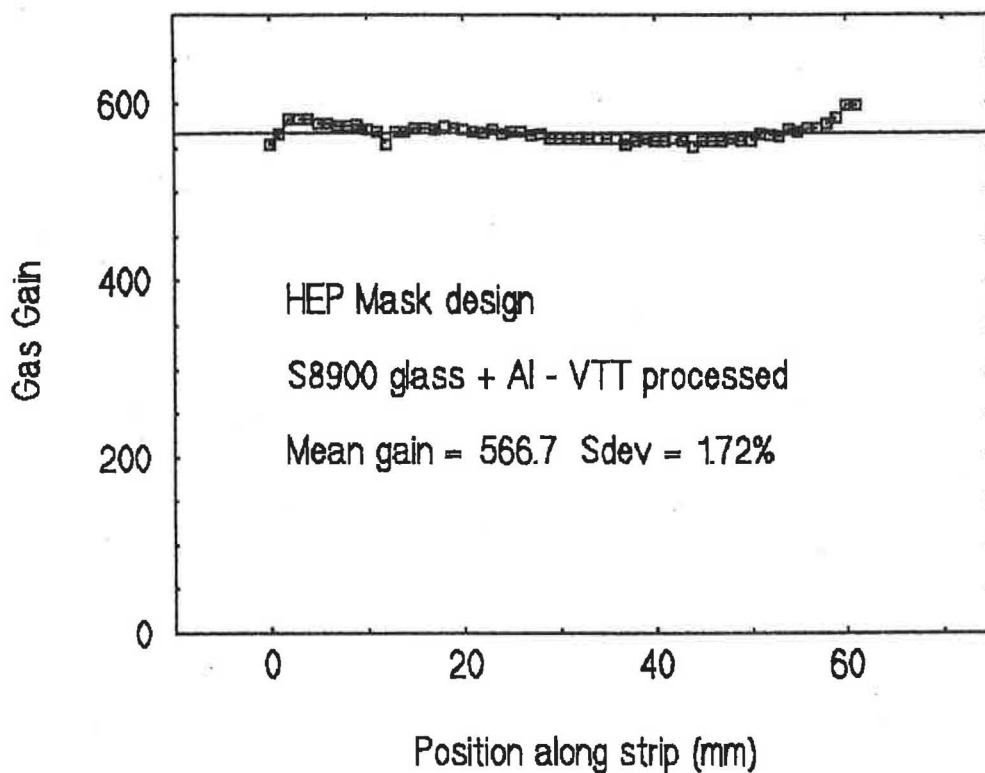


FIGURE 8

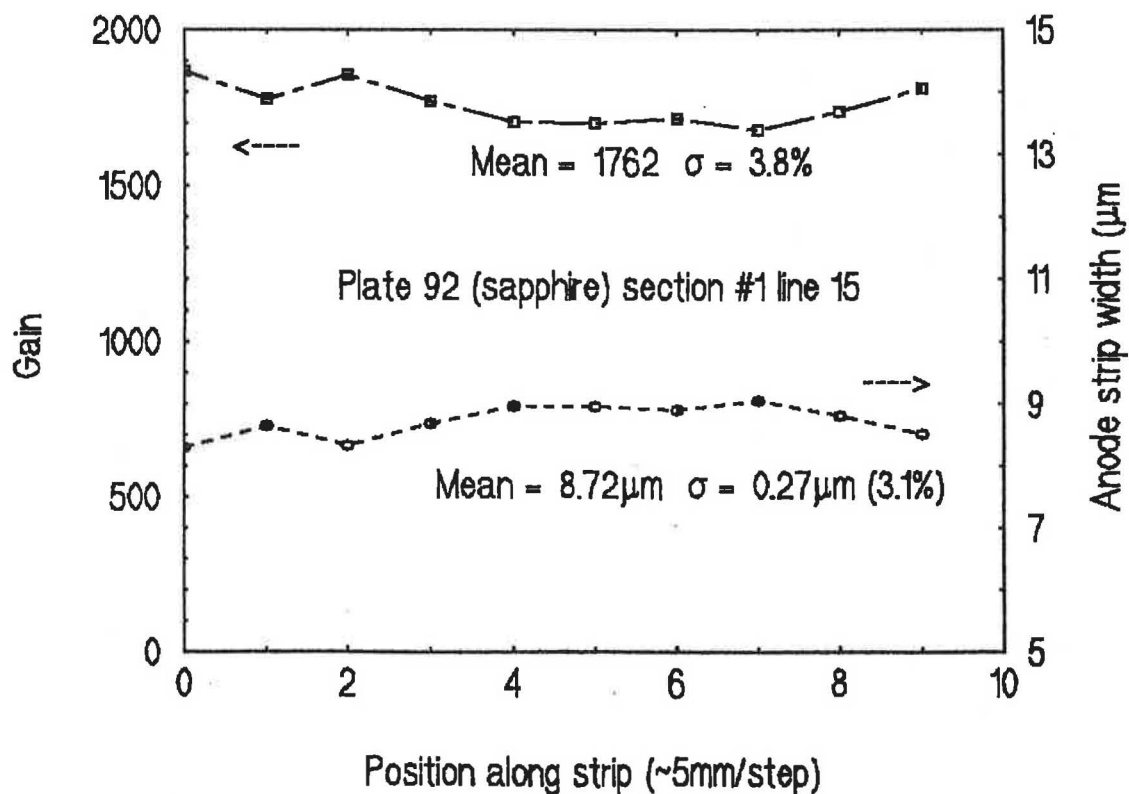


FIGURE 9

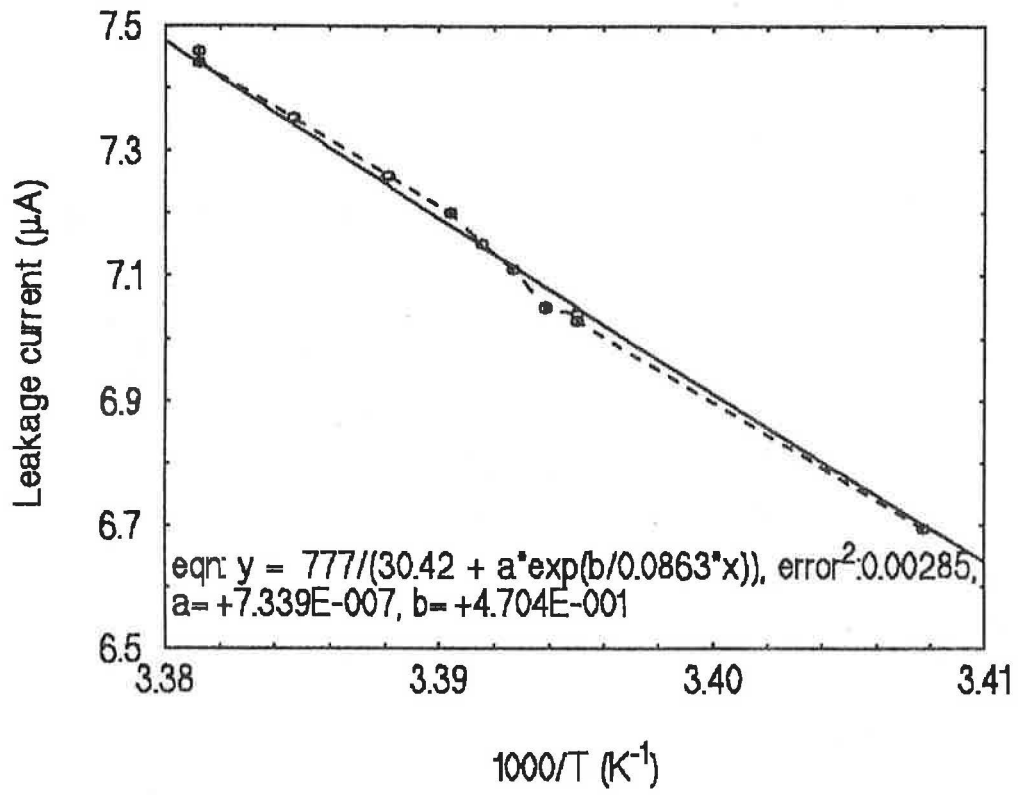


FIGURE 10

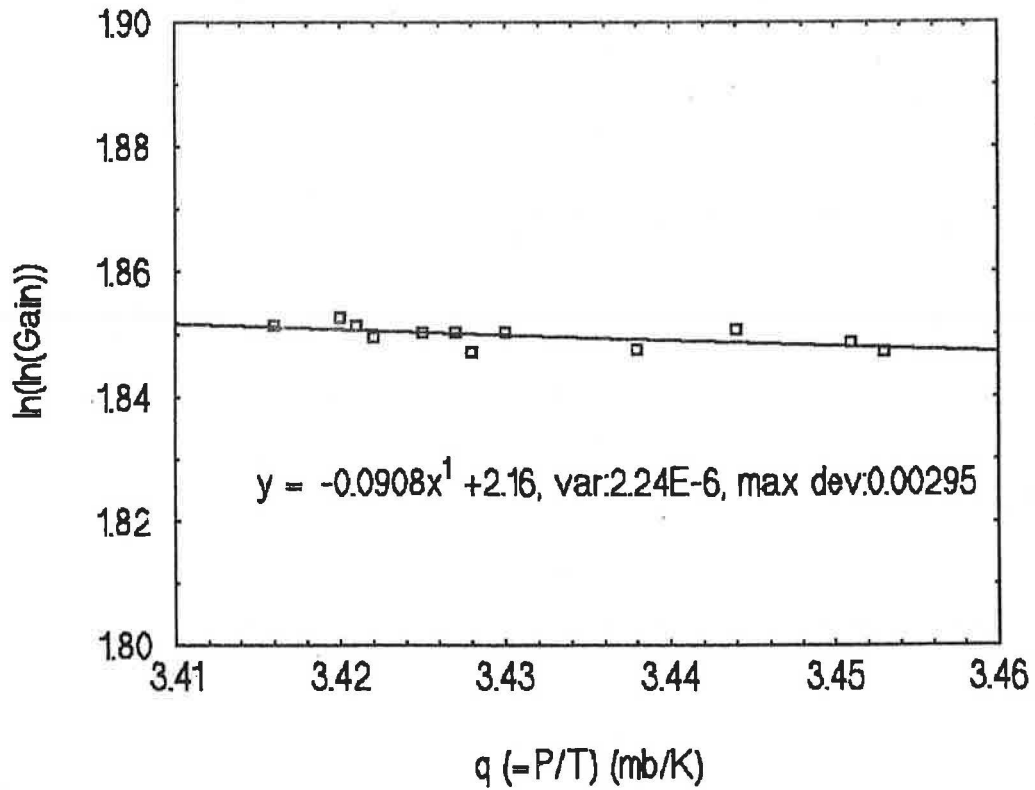


FIGURE 11

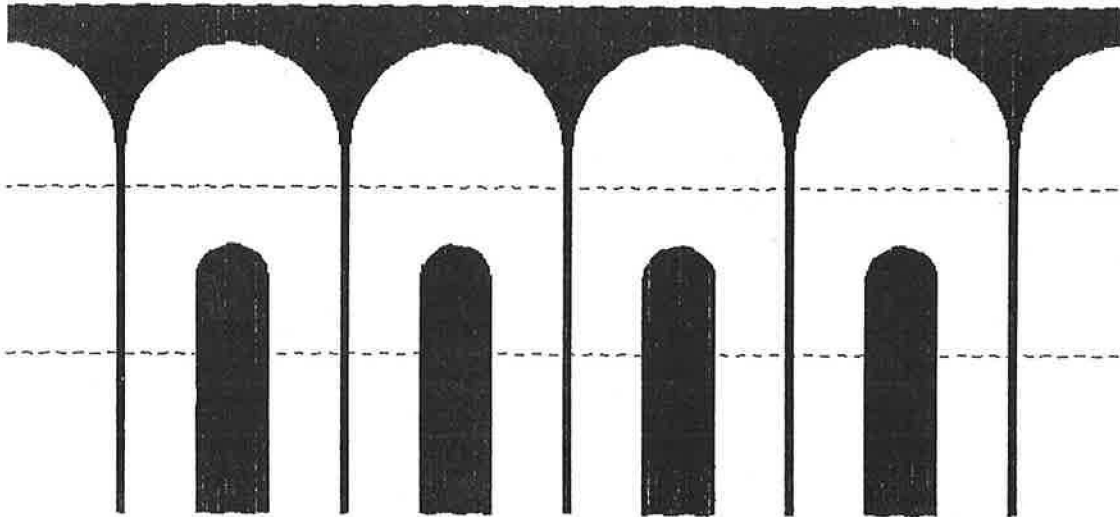


FIGURE 12

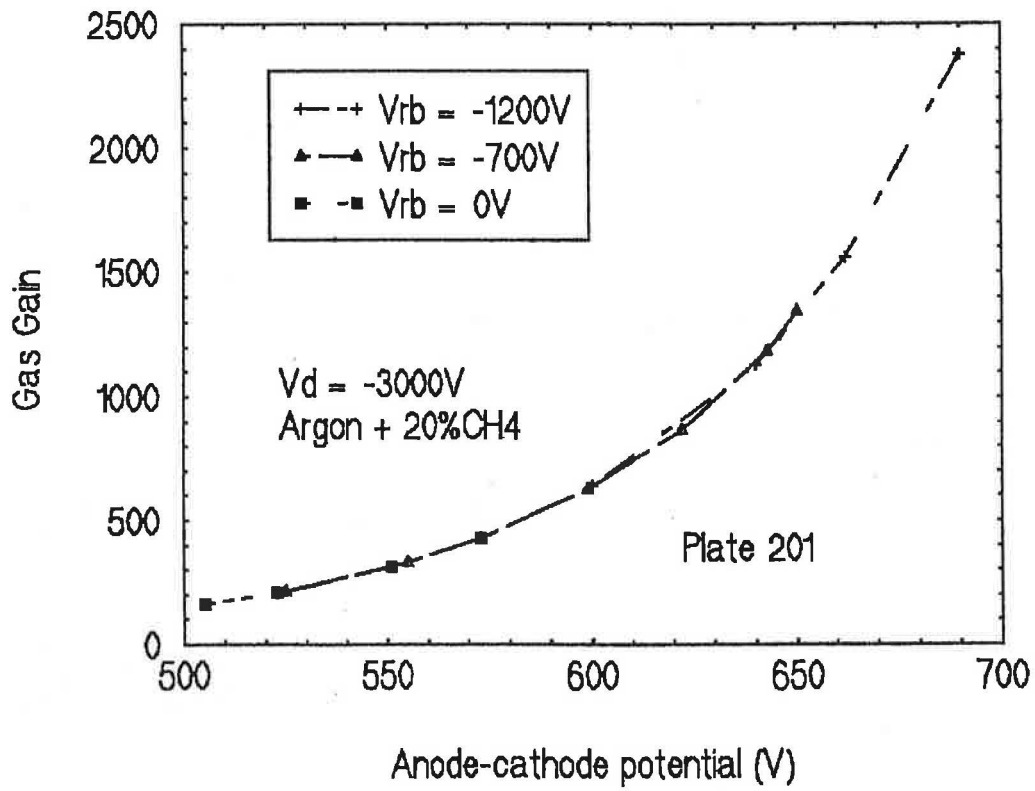


FIGURE 13

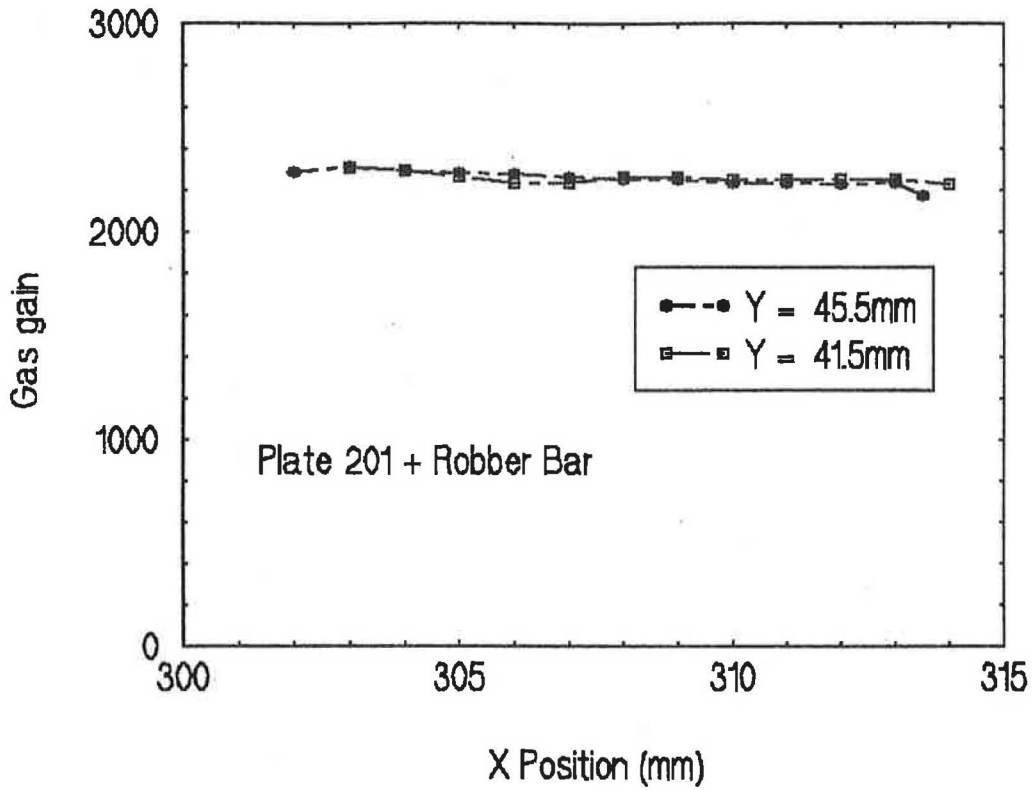


FIGURE 14

